Bull Earthquake Eng
DOI 10.1007/s10518-016-9878-7

ORIGINAL RESEARCH PAPER

Earthquake early warning scenarios at critical facilities in the Eastern Caribbean

Elisa Zuccolo[1] · Tony Gibbs[2] · Carlo G. Lai[1,3] · Joan L. Latchman[4] · Walter Salazar[4,5] · Luigi Di Sarno[2,6] · Anthony Farrell[2] · Lloyd Lynch[4] · Addison Workman[2]

Received: 31 July 2015 / Accepted: 29 January 2016

Abstract A feasibility study of an earthquake early warning (EEW) system was conducted for the Eastern Caribbean region using scenario earthquakes, corresponding to the maximum credible earthquakes and to the earthquakes associated with a return period of 475 years. Broadband synthetic seismograms were produced at selected critical facilities, where there is potential interest in the installation of an EEW system. The expected damage was derived from the synthetic seismograms and compared with the lead-time determined for both a regional and on-site EEW configuration. Next, the Virtual Seismologist EEW algorithm, as included in SeisComP3, was tested. Additional broadband synthetic seismograms were produced for the stations in the Eastern Caribbean seismic networks in order to simulate the real time behaviour of the seismic networks during the occurrence of the synthetic earthquakes and to assess the predictive capacity of the selected ground motion prediction equation. Expected peak ground parameters and lead-times at the critical facilities constitute the major outcome of the study.

Keywords Earthquake early warning · Eastern Caribbean · Earthquake scenarios · Synthetic seismograms

✉ Elisa Zuccolo
elisa.zuccolo@eucentre.it

1 Department of Civil Engineering and Architecture, University of Pavia, Via Ferrata 1, 27100 Pavia, Italy

2 Council of Caribbean Engineering Organisations, P. O. Box 715, Bridgetown BB11000, Barbados

3 European Centre for Training and Research in Earthquake Engineering, Via Ferrata 1, 27100 Pavia, Italy

4 Seismic Research Centre, UWI-The University of the West Indies, St. Augustine, Trinidad, Trinidad and Tobago

5 Faculty of Engineering and Architecture, Catholic University of El Salvador UNICAES, Santa Ana, El Salvador

6 Department of Engineering, University of Sannio, Piazza Roma, 21, 82100 Benevento, Italy

Published online: 10 February 2016

1 Introduction

The Eastern Caribbean is a region exposed to a medium to high seismic hazard, with a 475 years return period horizontal Peak Ground Acceleration (PGA) expected on stiff ground that ranges between 0.21 and 0.38 g (Bozzoni et al. 2011). The hazard is largely due to major subduction seismicity, which comprises both interface earthquakes located up to a distance of 300 km from the volcanic island arc and intraplate earthquakes with hypocentres down to a depth of about 200 km. The occurrence of large (MMaxObs 8.0–8.5, Shepherd 1992) and distant offshore earthquakes in the Eastern Caribbean, together with the existence of several critical facilities spread throughout the region that can benefit from an EEW system, makes the region well suited to assess the feasibility of an EEW system. The local critical facilities that can benefit of the EEW include hospitals/medical facilities, public utilities (e.g. electricity, water, telecommunications, sewerage), airports, sea ports and power plants (e.g. coal, bagasse, natural gas, oil, diesel oil, heavy oil, geothermal).

An EEW system uses information extracted from the first seconds of longitudinal (i.e. compression or P) waves to estimate the expected ground motion from an on-going earthquake and releases an alert prior to the arrival of the most damaging ground motion, represented by the transverse (i.e. shear or S) waves. The difference in arrival time between P- and S-waves is proportional to the distance from the hypocentre. The farther away a site to be protected is located from the epicentral region, the longer will be the warning time. However, the more distant the site is from the epicentre, the smaller is the intensity of ground shaking. As a result, the expected level of ground shaking may be insignificant in terms of damage potential, due to the attenuation of seismic waves in the lithosphere. Therefore, in assessing the utility of an EEW system, there is a trade-off between longer lead-time promoting effective warning and greater distance from the hypocentre reducing the need for such warning at the sites of interest.

Two main configurations are generally implemented: the regional (or network based) and on-site (or single station based) approaches. A hybrid approach (a combination of regional and on-site) also exists (e.g. Böse et al. 2008; Köhler et al. 2009; Zollo et al. 2010). In the regional approach, a network of stations is distributed on the territory, in proximity to the seismic sources. The regional EEW algorithms use the first P-wave arrivals detected at the network to estimate the magnitude and location of an earthquake and predict the ground motion at the (distant) site(s) to be protected using empirical ground motion prediction equations. The alarm (which travels at a speed much faster than S-waves since it is virtually close to the speed of light) is released based on expected damage at the target site(s), which is a function of ground shaking and vulnerability of the specific structure(s) to be protected. In the on-site approach, the stations are installed close to the target site. In this case, the EEW algorithm uses the parameters estimated over few seconds of recorded P-waves to estimate the ground motion at the same site and the expected time from the arrival of the potentially damaging S waves.

This work focuses on the results of a feasibility study of an EEW system by investigating whether such a system would be viable for selected sensitive facilities in the Eastern Caribbean. The feasibility study of the use of the EEW system was conducted using a two-step analysis, which involved:

1. Comparison of the theoretical warning times issuable to selected critical facilities with the expected damage;

2. Estimation of the accuracy and robustness of location and magnitude determined using the software package SeisComP3 (SC3, http://www.seiscomp3.org), which includes the regional Virtual Seismologist (VS) algorithm (Cua and Heaton 2007) for near-instantaneous estimates of earthquake magnitude [hereinafter referred to as VS(SC3)].

Both steps were carried out by:

(a) Identifying critical facilities potentially interested in an EEW system;
(b) Modelling scenario earthquakes (corresponding to the maximum credible earthquakes and to the earthquakes associated with a return period of 475 years), developing suitable velocity structural models and producing synthetic seismograms;
(c) Estimating the performance criteria and acceptable threshold limits relevant in seismic fragility analysis.

The selection of the sample of sensitive facilities, located in the Eastern Caribbean region and used in the present study, is discussed below.

2 Selection of critical facilities

Among the potentially vulnerable stakeholders spread throughout the islands, 11 facilities, in Antigua (Antigua and Barbuda), Barbados and Trinidad (Trinidad and Tobago), were chosen for this study. The selection was based on interviews and customized questionnaires distributed to administrators of hospitals/medical facilities, public utilities (e.g. electricity, water, telecommunications, sewerage), airports, sea ports and energy production plants (e.g. coal, bagasse, natural gas, oil, diesel oil, heavy oil, geothermal).

2.1 Antigua

Three critical facilities were identified in Antigua: Mount St John’s Medical Centre, V. C. Bird International Airport and Antigua Public Utilities Authority (APUA)—Water Plant. Mount St John’s Medical Centre is an hospital building, which is equipped with piped oxygen, an highly flammable gas. The oxygen is supplied to bedsides from a distribution unit acting under pressure; a complex network of ducts delivers the oxygen throughout the various buildings within the hospital complex. If appropriate sensors and shut-off valves were installed, the warning time provided by an EEW system may allow the oxygen supply to be interrupted, thus minimizing the probability of fires occurring. The critical element for V. C. Bird International Airport is the refuelling unit and storage facility. An EEW system may be used to discontinue the flow of fuel to the ramp locations using the ramp based switches. However, there are several switches and if they were all activated, the lines between them would remain filled with fuel that might still pose a danger if lines ruptured. Therefore, it would be safer to install the shut-off mechanisms on the lines feeding the ramp from the main storage. Thus, the supply to the ramp would be discontinued at the source. The third facility being considered is Antigua Public Utilities Authority (APUA)—Water Plant. This facility, although small, with a simple load bearing block walled building, provides an important service. It supplies water to the northern section of the island, where there are communities across the financial spectrum. There are some houses that do not have adequate private rainwater collection and distribution systems and they are critically dependent on the continuous supply from APUA. If the pumps were shut down by an EEW system, there would be less damage than if they were operating during an earthquake.

2.2 Barbados

Three critical facilities were also identified in Barbados: Grantley Adams International Airport Inc, Queen Elizabeth Hospital and Light & Power Plant Spring Garden. The main concern expressed at Grantley Adams International Airport was air traffic control. The scenario considered was the possibility of damage to the runway from a major earthquake. In that case, it may be desirable to abort the landing of in-coming flights and the take-off of those already taxing. Queen Elizabeth Hospital is the sole critical healthcare facility in Barbados. It was considered that, in case of an earthquake, a warning of a few seconds for the most severe seismic waves would promote safer operations of the hospital. The EEW device may be employed for the automatic shutdown of particularly vulnerable equipment. Such equipment would include the oxygen supply, incinerator, boiler and natural gas supply. The Light & Power Plant at Spring Garden provides the base load of electricity generation for the entire island. It was considered that, in case of an earthquake, a warning of a few seconds for the most severe seismic waves would be scarcely useful for the operation of the plant. The personnel at the Power Company believed that their facility would not benefit much from an EEW system.

2.3 Trinidad

The remaining five critical facilities were selected in Trinidad: Telecommunications Services of Trinidad and Tobago (TSTT), Water and Sewerage Authority (WASA), The National Gas Company (NGC) of Trinidad and Tobago Ltd, Point Lisas Industrial Port Development Corporation (PLIPDECO) and Petrotrin. TSTT is the oldest telephone company in Trinidad and Tobago. Communications would be essential in the aftermath of a large earthquake. While the idea of an EEW was considered potentially useful, it was difficult to identify specific modules that could be shut down with very short warning time. WASA manages the water and sewerage systems in Trinidad and Tobago. An EEW capability was considered very useful in shutting down systems with hazardous chemicals. NGC is a diversified state-owned company operating in the mainstream of Trinidad and Tobago's natural gas-based energy sector. The short time scales did not fully allow for the shut down of offshore platforms and critical valve station facilities. However it was considered that some warning was better than none. PLIPDECO is a port facility second only to the port of Port of Spain. The facility covers an area of 19.51 hectares. Here the EEW system would scarcely be useful. The main risk item would be the cargo cranes, which require a shut down time of 30 min. The Port Authority of Trinidad and Tobago (PATT) had a similar assessment. Petrotrin is an oil company located in the industrialised south Trinidad. Owned by the Government of Trinidad and Tobago there is a large risk exposure from earthquakes. An EEW system with short time scale would not allow full shut down of systems, however, the shut down process could at least get a head start. In general, the respondents in Trinidad and Tobago were very interested in EEW systems, but concluded that the time scales would only be useful for automatic actions.

3 Ground shaking scenarios

Broadband synthetic seismograms (0.1–25 Hz) were produced from 12 earthquake scenarios, using the broadband ground motion simulation method described in Crempien and Archuleta (2015), which uses an extended kinematic model of the seismic source with correlated random source parameters based on dynamic rupture models (Schmedes et al. 2013). A bilateral rupture nucleating in the middle of the fault was considered for all earthquake scenarios. To take into account the variability associated with the earthquake rupture, 10 different realizations of slip, rise time, peak time, and rupture velocity were considered for each scenario. The velocity models adopted were the average models defined by González et al. (2012) and the velocity model custom calibrated for Trinidad, Tobago and north-eastern Venezuela. Since the source function and the Green's functions are computed using a 1D approximation, it was decided to use the velocity model of the epicentre to characterize the source and consider the velocity model of the site as representative of the entire source-site path. The synthetic seismograms were produced both at the sensitive infrastructures and at the stations of the Eastern Caribbean seismic network. The Eastern Caribbean seismic network is formed by the TRN Network, which is managed by the Seismic Research Centre of The West Indies and comprises over 50 seismic stations strategically positioned on islands throughout the Eastern Caribbean, the network managed by the Institut de Physique du Globe de Paris (IPGP) in the French Antilles (Martinique and Guadeloupe), the network managed by the Fundación Venezolana de Investigaciones Sismológicas (FUNVISIS) in north-eastern Eastern Venezuela, the network managed by the Montserrat Volcano Observatory (MVO) in the island of Montserrat and the network managed by the Koninklijk Nederlands Meteorologisch Instituut (KNMI) in the Netherlands Antilles (Saba, St. Eustatius and St. Maarten). The maximum epicentral distance at which synthetic seismograms were produced was selected as a function of the rupture length, to maximise computer resources. Specifically, a maximum epicentral distance of 150 km was chosen for the earthquake scenarios with a rupture length <100 km, while a distance of 250 km was adopted for larger rupture lengths. The peak ground values found were compared with the two Ground Motion Prediction Equation (GMPE) of Zhao et al. (2006) and Kanno et al. (2006) to identify the GMPE that better matches the ground shaking in the Eastern Caribbean.

3.1 Earthquake scenarios

The earthquake scenarios for the three islands chosen were defined after a thorough analysis of the seismotectonic of the Eastern Caribbean, which is highly complex. As a result, multiple sources contribute to the hazard at a site.

Antigua lies along the eastern boundary of the Caribbean Plate, which is the Lesser Antilles subduction zone. The subduction (from east to west) of the Atlantic Ocean lithosphere under the Caribbean Plate generates both interface and intraplate earthquakes within the subducted North American Plate and a chain of active volcanoes along the island arc, from Grenada to Saba. Antigua belongs to the outer limestone Caribbees, which no longer manifest volcanism. The volcanic island arc lies about 300 km from the Eastern Caribbean trench, where the North American Plate begins to subduct beneath the Caribbean Plate with an average westward dipping angle of 50 degrees (Bengoubou-Valerius et al. 2008), generating large earthquakes of magnitude >8 (Salazar et al. 2013) down to about 200 km depth. Shallow focus earthquakes (depth $\leq$50 km) along the inclined interface seismic zone yields thrust focal mechanisms, while focal mechanisms of deeper intra-plate events (>50 km) indicate that there is normal faulting resulting from initial flexure of the down going Atlantic Slab. This area is known to have suffered several catastrophic earthquakes including the 8th February 1843 ($M_w \sim 8.5$ from Feuillet et al. 2011) megathrust event. The disaggregation of the probabilistic seismic hazard estimated in Bozzoni et al. (2011) was computed for the PGA and the 475-year return period. It suggests that hazard in Antigua is dominated by three different events. The first mode of the magnitude-distance distribution corresponds to an earthquake with M_w 7.25 and hypocentral distance 89 km, which can be associated with the intraplate seismogenic zone SZ4 (Bozzoni et al. 2011), while the other two modes, of comparable amplitudes, can be related to the shallow seismicity of the interface seismogenic zone SZ2 (Bozzoni et al. 2011). They are both located at an hypocentral distance of 31 km and have M_w 4.55 and M_w 6.25, respectively.

Barbados lies above the inclined interface subduction zone between the downward moving American Plate and the overriding Caribbean Plate. It differs geologically from other islands in the Eastern Caribbean since it does not have a magmatic origin, but represents the only sub-aerial section of the Barbados accretionary prism. The prism is the result of the off-scraping of sediment from the face of the downward moving North American plate and its accumulation along the hanging wall of the subduction zone. The maximum magnitude associated with the interface subduction zone is still debated. In fact, the maximum magnitude observed in the earthquake catalogue for the southern Lesser Antilles subduction zone is considered to be M_w 7 in Bozzoni et al. (2011, SZ3), but M_S 7.8 in Grases (1990). However, Gutscher and Westbrook (2009) suggested that a) the paucity of earthquakes observed in slow subduction zones is likely to be due to the long recurrence intervals between great events and b) slow subduction zones are capable of generating mega-thrust earthquakes ($M > 8.2$). For the disaggregation of the probabilistic seismic hazard, reference was made to the most updated disaggregation results of Salazar et al. (2013), which performed a probabilistic seismic hazard analysis focused on Barbados to include the possible occurrence of large, subduction, interface earthquakes of magnitude 8.0–9.0 that were not considered in Bozzoni et al. (2011). Results for the PGA and the 475-year return period indicate that hazard in Antigua is dominated by two different events: an interface earthquake with M_w 7.4 at a rupture distance of 42.5 km in the interface subduction zone SZ3 (Salazar et al. 2013) and an intraplate earthquake with M_w 8.0 at a rupture distance of 107.5 km in the subduction zone SZ5 (Salazar et al. 2013)

Trinidad is located on the south-east corner of the Caribbean plate, which is a broad zone of deformation characterized by a number of fault-bounded blocks engaged in a complex pattern of relative motion, with significant compression along the northern South American continental margin (Pindell et al. 2005; Pindell and Kennan 2009). Major strike-slip faults have been mapped in Trinidad, namely, the Northern-Range, Central Range, Darien Ridge, El-Pilar Fault, Arima Fault and Los Bajos Fault. Weber (2009) employed far and near field geodesy and palaeoseismology to search fossil earthquakes on the Central Range Fault, the principal active dextral strike-slip in Trinidad. He concluded that the Central Range fault was locked and stored and released significant elastic motion in the recent past, and that it could be locked today and might constitute a major seismic threat in Trinidad. He also suggested a slip rate of 12 mm/year and that several meters of motion may be stored in the fault. The maximum magnitude observed in the catalogue for the Trinidad faults is 6.6, however, a possible magnitude 7.7 is suggested by geodetic and paleoseismological investigations (Weber 2009). A dense area of seismicity, called Paria cluster, is also recognized NW of Trinidad (Russo et al. 1993). It includes shallow and intermediate events lying in a broad ENE-trending linear zone extending from the Gulf of Paria. These earthquakes deepen from the SE, in the Gulf of Paria, to the NW, where the deepest events attain depths of 200 km. The deeper (70–200 km) hypocentres define a steeply NW-dipping (60°) slab, which can be a subducting detached oceanic lithosphere and it represents one of the most active seismogenic sources in the Eastern Caribbean (Russo et al. 1993). The focal mechanisms suggest that normal faulting is occurring at the initial flexure of the down-going slab. However, mixed-motion earthquakes, with thrust and strike slip, support the interpretation that there is bending of the subducting slab at greater depths. The disaggregation of the probabilistic seismic hazard estimated in Bozzoni et al. (2011) was computed for the PGA and the 475-year return period for three representative sites closest to the five selected facilities. The three sites turn out to be characterized by two dominant modes: one is shallow with M_w 6.35 and hypocentral distance equal to 34 km and it is related to the crustal seismogenic zone SZ12, which includes the faults mapped in Trinidad (Bozzoni et al. 2011), the other is deep, with M_w 7.15 and hypocentral distances ranging from 109 to 129 km depending on the distance from the intraplate seismogenic zone SZ11 (Bozzoni et al. 2011).

Based on the considerations above, two sets of earthquake scenarios were modelled for each investigated island: two Maximum Credible Earthquakes (MCEs) and two earthquakes associated with the two dominant modes of the magnitude-distance joint distribution computed through the disaggregation analysis for PGA and the 475-year return period. For Antigua and Barbados, each set includes one interface and one intraplate earthquake, while for Trinidad a MCE for the Central Range Fault and a MCE for the intraplate seismicity associated with the Paria cluster were modelled.

In order to compute the fault dimensions from the selected magnitude, the empirical relationships by Blaser et al. (2010) and Strasser et al. (2010) specifically developed for subduction zones, were adopted. For a M_w 8.5 the orthogonal regression of Blaser et al. (2010) led to a rupture zone of 300 km length × 110 km width, consistent with that assumed by Feuillet et al. (2011) for the 8th February 1843 event; therefore, the relationships by Blaser et al. (2010) were used in this study to compute the fault dimensions of the interface scenario earthquakes. Instead, for the intraplate scenario earthquakes it was decided to use the empirical relationships by Strasser et al. (2010) specifically developed for intraplate events. For crustal events, the relationships by Wells and Coppersmith (1994) were considered. They led to a rupture length for the MCE for the Central Range Fault consistent with that assumed by Prentice et al. (2010): 50 km length onshore (Crosby et al. 2009) and at least 60 km offshore east of Manzanilla Bay (Soto et al. 2007).

The modelled scenarios are shown in Fig. 1, while their source parameters are described in Table 1.

3.2 Velocity structural models

The work by González et al. (2012) was used as reference for the definition of the velocity structural models selected for this study. It presents sets of S-wave velocity structural models of the Caribbean with a resolution of 2° × 2°, determined from the inversion of Rayleigh wave group velocity dispersion and defined down to a depth of 300 km. For each 2° × 2° cell a range of variability for the thickness (h) and shear-wave velocity (Vs) of each layer is given. In the present analytical work, the velocity models associated with the average values assigned to the cells covering the Eastern Caribbean were taken into account. They are shown in Fig. 2a. The P-wave velocity (V_P) was computed from Vs

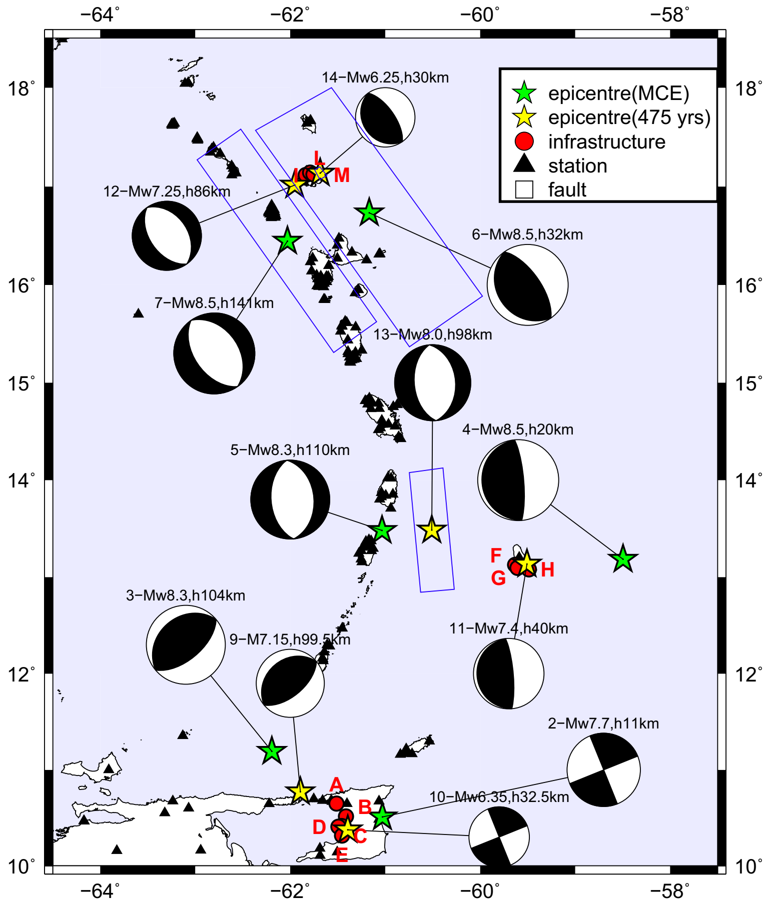

Fig. 1 Earthquake scenarios (epicentres—stars, surface projection of fault planes—empty rectangles, focal mechanisms—beach balls; the magnitude and focal depth of each earthquake are shown above each beach ball). The *black triangles* denote the seismic stations, while the *red circles* indicate the selected critical facilities: *A* Telecommunications Services of Trinidad and Tobago (TSTT) Head Office, *B* Water and Sewerage Authority (WASA) Central Office, *C* National Gas Company (NGC), *D* Port of Point Lisas Industrial Port Development Corporation (PLIPDECO), *E* Petrotrin Head Office, *F* Light & Power Plant Spring Garden, *G* Queen Elizabeth Hospital, *H* Grantley Adams International Airport Main Terminal, *I* Mount St. John's Medical Centre, *L* V.C. Bird International Airport, *M* The Antigua Public Utilities Authority (APUA)

assuming a ratio of $\sqrt{3}$, the density was estimated from the the Nafe-Drake curve (Ludwig et al. 1970) and quality factors were determined based on Olsen et al. (2003).

An ad-hoc calibration was performed for Trinidad and Tobago and north-eastern Venezuela, based on a systematic comparison between recorded and synthetic time histories. Recorded time histories were retrieved from the strong motion database for the Eastern Caribbean Islands (Salazar 2012), while the synthetic time histories were produced according with the modal summation technique using the suite of programs "Computer Programs in Seismology—Version 3.30" developed by Herrmann (2003). Seven sets of time series recorded at the TBH station (10.49580N, 61.06790W), which is located on

Table 1 Source parameters for the considered earthquake scenarios (*F* interface, *P* intraplate, *C* crustal)

Island	Scenario	Reference SZ	M_w	Strike (°)	Dip (°)	Rake (°)	Focal depth (km)	Length × width (km)
Antigua	MCE (F)	–	8.5[1]	145[6]	24[9]	90[12]	32[14]	300 × 110[18]
	MCE (P)	SZ4[B]	8.5[2]	145[6]	50[9]	270[13]	141	267 × 93[19]
	475 years (F)	SZ2[B]	6.25[3]	145[6]	24[9]	90[12]	30[15]	15 × 10[18]
	475 years (P)	SZ4[B]	7.25[3]	145[6]	50[9]	270[13]	86[15]	53 × 33[19]
Barbados	MCE (F)	–	8.5[4]	175[6]	11[4]	90[12]	20	300 × 110[18]
	MCE (P)	SZ5[B]	8.3[2]	175[6]	50[9]	270[13]	110	206 × 79[19]
	475 years (F)	SZ3[S]	7.4[3]	175[6]	10.5[10]	90[12]	40[16]	70 × 35[18]
	475 years (P)	SZ5[S]	8.0[3]	175[6]	50[9]	270[13]	98[15]	140 × 61[19]
Trinidad	MCE (C)	–	7.7[5]	68[7]	90[11]	180[11]	11[17]	124 × 21[20]
	MCE (P)	SZ11[B]	8.3[2]	50[8]	60[8]	90[8]	104	206 × 79[19]
	475 years (C)	SZ12[B]	6.35[3]	68[7]	90[11]	180[11]	32.5[15]	20 × 9[20]
	475 years (P)	SZ11[B]	7.15[3]	50[8]	60[8]	90[8]	99.5[15]	46 × 30[19]

[B] Bozzoni et al. (2011), [S] Salazar et al. (2013), [1] from Feuillet et al. (2011) in order to model a 8th February 1843-like event, [2] maximum magnitude of the associated SZ, [3] from the disaggregation analysis, [4] from Gutscher and Westbrook (2009), [5] from Weber (2009), [6] azimuth of the trench, [7] from Weber et al. (2001), [8] from Russo et al. (1993), [9] from Bengoubou-Valerius et al. (2008), [10] from Salazar et al. (2013), [11] assumption of pure right lateral—strike slip focal mechanism, [12] assumption of pure reverse focal mechanism, [13] assumption of pure normal focal mechanism, [14] computed based on the epicentre proposed by Feuillard (1985) (Lon: 61.17W, Lat: 16.73N) and a 10-km-depth updip limit, [15] mean depth of the associated SZ, [16] estimated by modelling SZ3 as an inclined plane, dipping to the west at an angle of 10.5°, with the trench located at 57.529W and a maximum depth of 50 km at 60W, according with Salazar et al. (2013),[17] computed with a 0.5-km-depth updip limit according with Prentice et al. (2010), which suggested that surface rupture occurred on the Central Range Fault in the late Holocene, most recently between 2710 and 550 years B.P.,[18] from Blaser et al. (2010), [19] from Strasser et al. (2010), [20] from Wells and Coppersmith (1994)

Table 2 Main characteristics of the events recorded at TBH station

No.	Date	Time	Epicentral coordinates	Depth (km)	M_W	Strike (°)	Dip (°)	Rake (°)	Epicentral distance (km)
1	2000/10/04	14:37:45	11.15N 62.48W	110.4	6.1	277	42	141	170.2
2	2003/06/21	05:55:57	10.79N 59.27W	10.0	5.3	253	76	12	198.8
3	2004/12/02	19:16:32	10.49N 61.45W	48.2	5.8	89	13	−21	41.7
4	2004/12/03	03:46:44	10.54N 61.46W	40.5	5.4	228	40	−90	43.1
5	2005/10/24	09:19:16	11.10N 62.39W	137.7	5.1	279	46	159	159.0
6	2005/10/28	22:30:58	11.11N 62.04W	80.9	5.5	4	9	−154	126.0
7	2006/09/29	18:23:06	10.79N 61.75W	52.8	5.5	11	57	−178	81.3

rock, were used. The main characteristics of the recorded events are listed in Table 2, while Fig. 3 shows the location of the TBH station and of the epicentres of the earthquakes used in the analysis.

An initial model was defined based on the work of González et al. (2012), using the average values assigned to the cell W-62N10. For greater depths (down to about 1000 km),

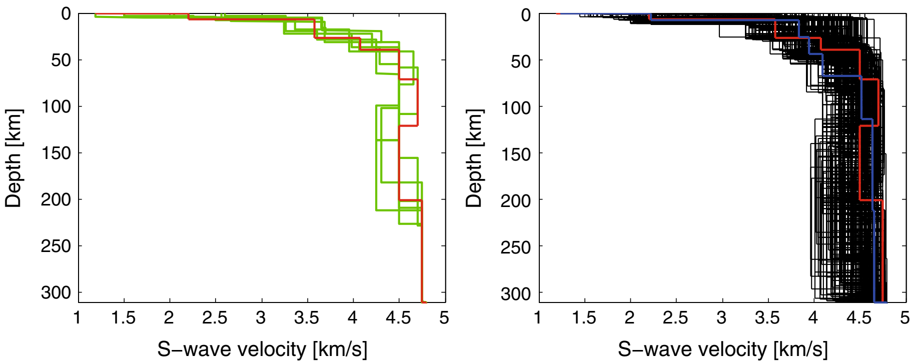

Fig. 2 (*Left*) Vs versus depth models down to 310 km defined by González et al. (2012) for the Eastern Caribbean region (average models, *green lines*); the velocity model for Trinidad and Tobago and North-Eastern Venezuela is highlighted in *red*; (*right*) Vs versus depth models (*black lines*) down to 310 km derived through random perturbations of the thickness and S-wave velocity of the initial velocity model for Trinidad and Tobago and North-Eastern Venezuela (*red line*); the "best" velocity model is highlighted in *blue*

the global 1D model AK135 (Kennett et al. 1995) as prepared for use in Computer Programs in Seismology (http://www.eas.slu.edu/eqc/eqc_cps/TUTORIAL/SPHERICITY/) was used. The overall model was implemented by merging the two models mentioned and appropriately modifying the Vs of the boundary layer of the model AK135 in order to avoid the generation of an artificial low-velocity layer. To identify the structural model giving the best fit to all the recordings used, different velocity models were tested. They were created from the one previously defined and randomly varying h and Vs of each of the uppermost layers (down to 310 km). Three sets of 99 velocity models were generated by varying h and Vs of a random number independently chosen within the interval [−10 %, +10 %] with respect to the value (h or Vs) assumed in the previous cycle. For each set, 99 cycles were considered, for a total of 298 velocity models. They are shown in Fig. 2b. Possible errors in the estimation of source parameters were catered for by using 243

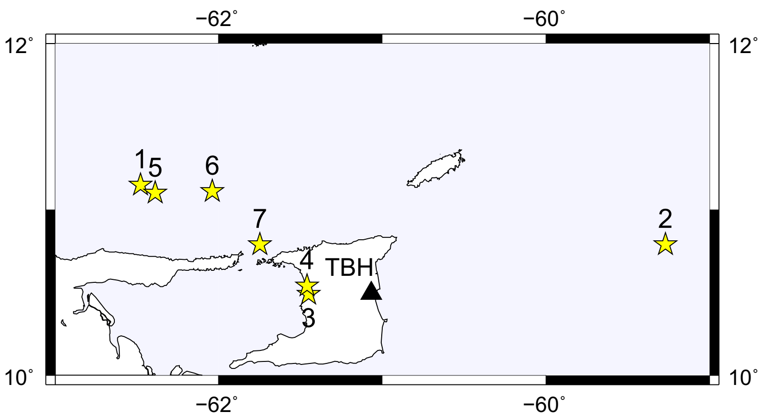

Fig. 3 Location of the TBH station (*black triangle*) and of the seven earthquakes used for the calibration of the velocity model for Trinidad and Tobago and North-Eastern Venezuela (*yellow stars*)

combinations of source parameters for each set of recordings. They were obtained by varying the magnitude (±0.1), the focal mechanism (strike ± 10°, dip ± 10°, rake ± 10°) and the focal depth (±20 %). Both synthetic and recorded time series were bandpass filtered using a 10th-order Butterworth filter with a low cutoff frequency chosen independently for each recording, according to the frequency adopted in the correction of the signals (Salazar 2012). The high cutoff frequency was fixed at 1 Hz.

The misfit between observed and synthetic time histories was estimated using the goodness-of-fit (GOF) test developed by Olsen and Mayhew (2010). Among the different metrics commonly used to describe ground-motion time series, the Fourier spectrum (smoothed to reduce variance) was chosen herein. The GOF value was determined within the frequency range used for filtering the signals. The "best model" was considered to be the one giving the highest average GOF, where the average was determined using the seven events considered (for each event the GOF was determined as the average of the GOFs associated with the 3 components of motion—NS, EW and vertical). The "best" fitting model, associated with an average GOF value of 56.6 ('fair fit' according with the GOF classification by Olsen and Mayhew 2010), is shown in Fig. 2b. The comparison between recorded and synthetic velocity time series produced with the "best" model is shown in Fig. 4. As enhanced by the GOF values listed in Table 3, the simulation matches the recorded data satisfactorily. In fact, at least one ground motion component has a GOF $\sim$ 60.0 or above (i.e. close to the threshold of a 'very good fit', GOF = 65).

The spatial variability of the adopted velocity models was quantified through the shear-wave velocity coefficient of variation as a function of depth, which exhibits large values (19–36 %) in the upper 5 km and values less than 6 % for depths greater than 25 km.

4 Damage threshold values

A comprehensive review of the state-of-the-art was undertaken to determine reliable threshold values of ground motion intensity measures for the EEW alerts. A number of studies dealing with the definition of allowable acceleration values exist (e.g. Chong and Soong 2000; Goodwin et al. 2004; Chaudhuri and Hutchinson 2006; Retamales et al. 2008; Konstantinidis and Makris 2009), although the outcomes of such studies, which were derived primarily from post-earthquake survey and shake-table tests, may appear controversial. Additionally, the application of the existing alert thresholds is generally limited to single mechanical, electrical and medical units. Systemic approaches are needed, as it is essential to convolute the vulnerability of the components of the system under consideration for a reliable estimation of the threshold alert values.

The response parameters were given for three limit states that characterize the seismic behavior of the sample structures and infrastructures: slight, moderate and severe damage. To determine the threshold limits, the ultimate limit state (ULS) was considered as a reference. At that stage, there is severe damage, which implies that the structure can still bear the gravity loads, but is near collapse for horizontal loads. Moderate damage corresponds to nearly half of the response parameters at ULS, while slight damage is about 1/3 of the peak demand parameters at ULS.

For most of the critical facilities identified in Antigua, Barbados and Trinidad, the alert response was expressed in terms of PGA, at the site, since the vulnerable components included in the case study facilities are usually acceleration-sensitive. The values of the PGA estimated for the severe damage limit state were derived from the maximum floor

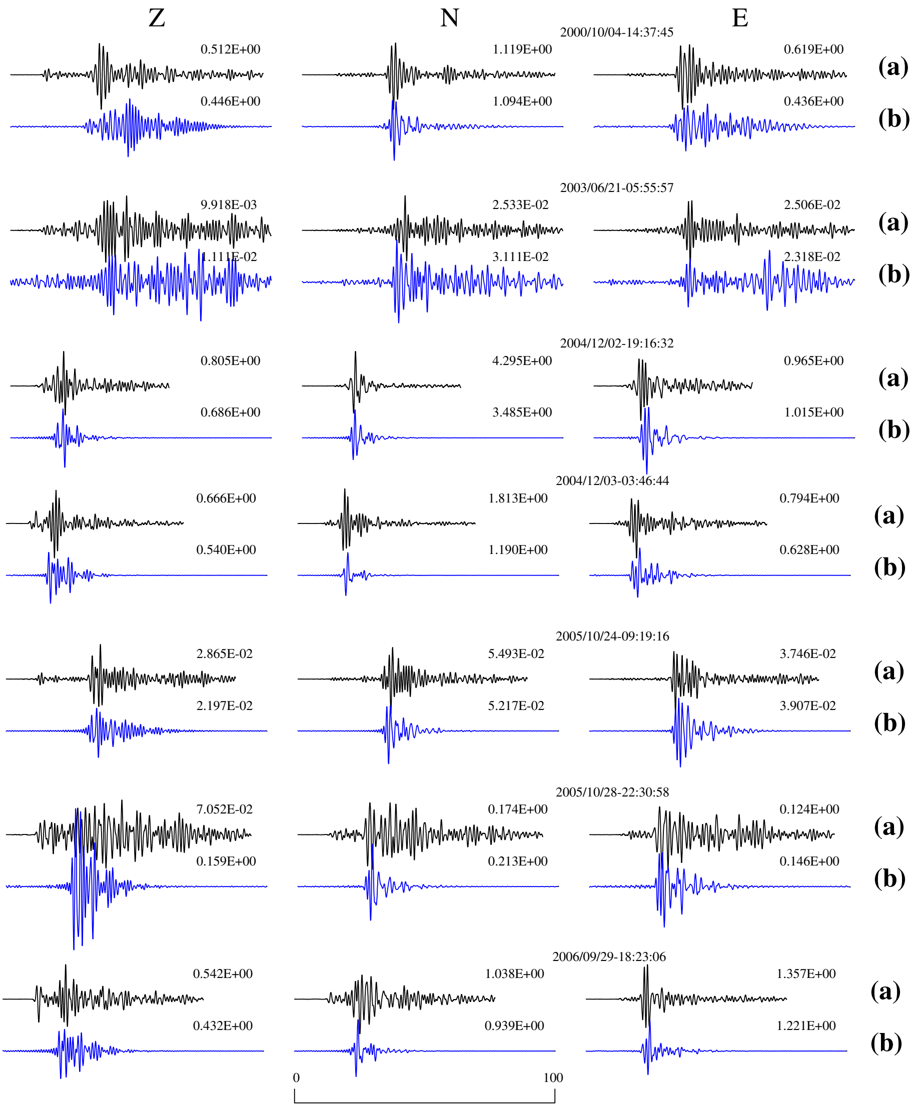

Fig. 4 Comparison between the three-component recorded (*a*, *black lines*) and synthetic (*b*, *blue lines*) velocity time histories associated with the seven earthquakes used for the calibration of the velocity model for Trinidad and Tobago and North-Eastern Venezuela. All the recordings are filtered to 1 Hz. Trace amplitudes are in cm/s. *Left* vertical component, *middle* NS component, *right* EW component

acceleration of the buildings and then converted to PGA adopting a 2.5 dynamic amplification, which is considered realistic for the sample structures. Further refinement is, however, possible if the geometric and mechanical properties of the buildings are known, along with the lateral-resisting system, if any.

For the gas pipelines of the National Gas Company of Trinidad and Tobago Ltd, the alert response parameter was expressed in terms of PGV. PGV was found critical in comprehensive studies dealing with the seismic risk of pipelines transporting and

Table 3 GOF values for each waveform obtained with the "best" model

Event	Average GOF	Ground motion component		
		Z	NS	EW
1	54.7	51.4	48.3	64.4
2	50.2	61.6	45.5	43.4
3	66.6	56.0	69.8	74.1
4	49.4	43.9	43.5	60.9
5	61.0	63.6	61.0	58.4
6	58.7	58.5	57.9	59.8
7	55.7	57.0	45.9	64.4

The GOF classification proposed by Olsen and Mayhew (2010) is: 0–35 bad fit, 35–45 poor fit, 45–65 fair fit, 65–80 very good fit, 80–100 excellent fit

distributing natural gas for industrial and civil use (e.g. O'Rourke and Liu 1999; O'Rourke and Deyoe 2004; Tromans 2004; Lanzano et al. 2013). The damaging effects due to the passage of seismic waves in the soil are proportional to the PGV; thus the latter parameter can be reliably utilized to monitor possible damage to gas pipelines when their integrity is of concern.

The fragility curves adopted for the sample critical infrastructures are summarized in Table 4, along with the threshold values. The threshold values for the critical structures, namely the hospitals, the airport control towers and the headquarter buildings, depend on numerous factors, e.g. material of construction, structural system and building use and occupancy. The curves proposed by Pitilakis et al. (2014) were used as references as they are considered sound and rely on extensive numerical simulations. However, such fragility curves do not exist for the various critical structures considered herein. Thus, the curves proposed for hospitals were assumed realistic as representative of the response of the airports (control towers were assumed as critical for the Grantley Adams International Airport Main Terminal in Barbados and the V.C. Bird International Airport in Antigua and Barbuda) and the response of the headquarter buildings (e.g. Antigua Public Utilities Authority, Telecommunications Services of Trinidad and Tobago, Water and Sewerage Authority Central Office and Petrotrin Head Office). The formulation by Lanzano et al. (2013) was used for the response of the pipelines of the NGC in Trinidad and Tobago. For the case of the Light & Power Plant in Barbados, the reference values provided by Porter and Kiremidjian (2001) were utilized. The approach considered the stress on the whole

Table 4 Fragility functions and threshold levels used for the selected critical facilities

Island	Critical facility	Fragility curves	Threshold level (PGA or PGV)		
			Slight	Moderate	Severe
Antigua	Hospital/Airport	Pitilakis et al. (2014)	0.27 g	0.4 g	0.8 g
	APUA	Pitilakis et al. (2014)	0.17 g	0.25 g	0.5 g
Barbados	Hospital/Airport	Pitilakis et al. (2014)	0.27 g	0.4 g	0.8 g
	Light & Power Plant	Porter and Kiremidjian (2001)	0.2 g	0.3 g	0.6 g
Trinidad	TSTT/WASA/Petrotrin	Pitilakis et al. (2014)	0.27 g	0.4 g	0.8 g
	PLIPDECO	Pitilakis et al. (2014)	0.2 g	0.3 g	0.6 g
	NGC	Lanzano et al. (2013)	45 cm/s	90 cm/s	120 cm/s

Threshold levels refer to a C/D site classification according to the NEHRP (BSSC 2003) facility as a convolution of the fragility of the single most vulnerable components. As such, the response of switch gears and transformers was of primary importance.

5 Expected damage and theoretical lead-times

The utility of an EEW system was defined in terms of expected damage and theoretical lead-time.

The expected damage was assessed for each couple facility-earthquake scenario, based on the maximum horizontal component of the peak ground motion parameter (either PGA or PGV) determined at each critical facility, averaged between the 10 different source realizations associated with each earthquake scenario. To promote conservatism, the average PGA/PGV value increased by one standard deviation was also adopted. In an attempt to compensate for limitations in available geotechnical information for the selected sites, the peak values found for hard rock were converted into peak values on a NEHRP (BSSC 2003) site class D using specific site coefficients. They were defined as the ratio between the site coefficients for soil class D ($V_{S30} = 250$ m/s) and hard rock ($V_{S30} = 1100$ m/s) (Kanno et al. 2006).

The theoretical lead-time (i.e. the available time to implement safety measures before the arrival of the potentially damaging seismic waves at the sites of interest) was estimated for the selected critical facilities simulating both a regional and an on-site EEW configuration. The regional lead-times were computed considering 6 stations to be triggered in order to have a reliable estimate of magnitude, hypocentre and origin time of the earthquake, according with the minimum detections required by VS(SC3). However, the 6 triggering stations requirement is only a legacy of SeisComP3's standard location algorithm that will be overcome in future (Behr, personal communication). In fact, there exist several algorithms that can estimate magnitude and epicentral location starting from the first one or two P-wave recordings (e.g. Cua 2005; Satriano et al. 2008; Meier et al. 2015). Although none of the existing algorithms may currently work in real-time in the Eastern Caribbean, regional lead-times were computed considering also a 2-station trigger, in order to give an idea of the lead-times that could be obtained in future. Travel times of P- and S-waves to the seismic stations and the critical facilities were estimated using theoretical paths from geometrical optics. The suite of programs "Computer Programs in Seismology—Version 3.30" developed by Herrmann (2003) and the structural velocity models adopted for the production of synthetic seismograms were used for this purpose.

For the regional configuration 5 s of technical times were considered. They include 1 s for sending the results to the processing centre, 3 s for actual data processing and 1 s for the transmission of the warning message (Allen 2007; Behr et al. 2015). Of course, these values are strongly dependent on the selected algorithm, technology and on the characteristics of the seismic stations. For the on-site configuration 3 s of technical times (processing time) were used (i.e. Kanamori 2005; Wu and Kanamori 2005). The results of such analyses are summarized in Table 5. A 5-s lead-time can be assumed as the minimum time interval sufficient for shutting-down essential, automatized processes controlling the operations in critical structures, such as hospitals, airports and headquarter buildings. However, longer lead-time, order of magnitude 10–15 s, are deemed necessary to shut-down essential operations in the facilities that are of interest in the current feasibility study. Yet, this lead-time may still vary significantly depending on the specific features of the investigated facility.

Table 5 Expected damage and theoretical lead-time for each couple critical facility-earthquake scenario considered (*F* interface, *P* intraplate, *C* crustal)

Island	Scenario	Expected damage	Lead-time regional (6-station trigger) (s)	Lead-time regional (2-station trigger) (s)	Lead-time on-site (s)
Antigua	475 years (F)	Nil (hospital) Nil/slight (airport) Slight/moderate (APUA)	NA	NA	1–2
	475 years (P)	Nil (hospital and airport) Slight (APUA)	5	5	7
	MCE (F)	Slight/moderate (hospital and airport) Moderate/severe (APUA)	9–10	9–11	7–8
	MCE (P)	Slight/moderate (hospital and airport) Moderate (APUA)	15	15	14
Barbados	475 years (F)	Severe (hospital, airport, APUA)	NA	0–1	2
	475 years (P)	Slight/moderate (airport) Moderate (hospital) Moderate/severe (Light & Power Plant)	13–16	14–17	12–13
	MCE (F)	Moderate (hospital and airport) Moderate/severe (Light & Power Plant)	NA	7–11	10–12
	MCE (P)	Slight/moderate (hospital and airport) Moderate (Light & Power Plant)	25–29	26–29	17–18
Trinidad	475 years (C)	Nil (TSTT and NGC) Nil/slight (WASA) Slight (Petrotrin) Slight/moderate (PLIPDECO)	NA–0	NA–1	1–3
	475 years (P)	Nil (TSTT, NGC, WASA, Petrotrin) Slight (PLIPDECO)	6–9	8–11	9–10
	MCE (C)	Nil/slight (TSTT) Moderate (WASA) Severe (PLIPDECO, Petrotrin, NGC)	NA–1	4–8	3–4
	MCE (P)	Slight (NGC) Slight/moderate (Petrotrin) Moderate(TSTT, WASA, PLIPDECO)	10–16	12–18	12–14

5.1 Antigua

The damage expected for the 475-year return period is near nil in the case of Mount St John's Medical Centre and V.C. Bird International Airport, for which the damage thresholds are higher (see Table 4), and is slight (or even moderate for APUA). Therefore there would be no utility in an EEW system for the hospital and the airport. However, it could be possibly useful for APUA. The interface scenario is characterized by close proximity to the facility considered and, as a result, APUA was found to be located in the blind zone. The intraplate scenario is also characterized by close (epicentral) distance to APUA, but its focal depth is greater and therefore a regional lead-time of 5 s is possible. The on-site lead-time was found to be 7 s, i.e. 2 s larger than the regional lead-time. This arises from the hypocentre being located offshore and therefore, in the case of a regional EEW, the seismic waves would have to arrive at stations in Montserrat before the earthquake could be located. For the MCEs, the expected damage is slight/moderate for the hospital and the airport, moderate or even severe for APUA. The theoretical lead-time is about 9–11 s for the interface scenario and about 15 s for the intraplate scenario; therefore an EEW system may be useful in these cases. The regional lead-times do not vary significantly using 6 or 2 triggering stations. The lead-times for Antigua strongly depend on the location of the earthquakes and their distance from the island. If the epicentre is located near Montserrat or Guadeloupe, long lead-times (>10 s) can be possible for a regional EEW configuration. On the other hand, if the epicentre is located near Antigua or in an easterly direction far away from Guadeloupe, the lead-times for a regional configuration are lower and possibly less than those associated with an on-site EEW configuration. Therefore, it may make more sense to use an on-site algorithm combined with a regional algorithm. For example, PreSEIS (Pre-SEISmic shaking) is a neural network-based approach to EEW that takes advantage of both regional and on-site early warning (Böse et al. 2008; Köhler et al. 2009).

5.2 Barbados

In the case of Barbados, the damage expected for the interface scenario associated with the 475-year return period is severe for all the three facilities; however, the facilities lie within the blind zone for the regional EEW configuration and, therefore, no useful lead-time is possible. For the intraplate scenario associated with the 475-year return period, the expected damage ranges from slight/moderate for the Grantley Adams International Airport to moderate/severe for the Light & Power Plant, with relevant lead-times, both for the regional (13–17 s) and the on-site EEW configuration (12–13 s). The intraplate MCE has a magnitude slightly larger than that of the intraplate 475-year return period earthquake and it is located farther away from Barbados; therefore, the associated damage is similar to that expected for the 475-year return period: slight/moderate for the Queen Elizabeth Hospital and the airport and moderate for the Light & Power Plant. The greater distance also affects the associated lead-times, which are found to be very long. Since the epicentre is situated offshore, but between Saint Lucia and St. Vincent, the estimated lead-times for a regional EEW configuration (25–29 s) are about 10 s longer than those found for an on-site EEW configuration (17–18 s). For the interface MCE, the expected damage is moderate for the three facilities considered, or possibly severe for the Light & Power Plant. In this case, the epicentre is located offshore in an easterly direction far away from all the other islands. Since only four stations (i.e. less than the minimum number of P-waves detections required by VS algorithm) are operating in Barbados, the facilities lie within the blind zone for the regional EEW configuration with 6-triggering stations. Therefore the on-site EEW configuration currently represents the only choice, with lead-times of 10–12 s. Instead, considering only 2 triggering stations, the critical facilities would no longer be localized in the blind zone, but a regional lead-time of 7–11 s would be possible. Summing up, the PGAs and lead-times found suggest that the installation of a hybrid EEW system at the sites tested in Barbados would be useful.

5.3 Trinidad

The damage expected for the crustal scenario associated with the 475-year return period ranges from nil (for TSTT and the NGC) to slight/moderate (for PLIPDECO), depending on the distance from the modelled source. Most of the facilities lie within the blind zone for the regional EEW configuration; therefore, no useful lead-time is possible in this case. For the intraplate 475-year return period earthquake, the expected damage is nil for most of the facilities, except for PLIPDECO, where it is slight; therefore, the installation of an EEW system may be unnecessary. When the crustal MCE is considered, the expected damage ranges from nil/slight (for TSTT) to severe (for PLIPDECO, Petrotrin and NGC). Even if an EEW system were desirable due to the strong shaking expected, the facilities are located close to the hypocentre, and thus the associated lead-times are very low (NA–1 s for the regional EEW with 6 triggering stations and 3–4 s for the on-site EEW configuration). However, utilizing only 2 triggering stations, the regional lead-times would be higher (6–7 s for the three facilities for which a severe damage is expected). For the intraplate MCE, the expected damage is largely moderate for most of the facilities (except for NGC, for which it is slight) and the associated lead-times are significant (10–18 s for the regional EEW, 12–14 s for the on-site EEW). Summing up, a regional EEW is recommended for the strong intraplate seismicity associated with the Paria cluster. The simulations performed do not justify, at present, the installation of an EEW system (on-site or regional with 6 triggering stations) to detect earthquakes generated from the shallow active faults in Trinidad. In future, when a 2-station trigger algorithm will work in real-time, the installation of a regional EEW aimed at protecting facilities even from strong crustal earthquakes should be assessed in relation to the small operational lead-times allowed (<8 s).

6 Testing of VS(SC3) with synthetics

The lead-times given in Table 5 were found without taking into account any EEW algorithm able to estimate the magnitude and hypocentral location of an on-going earthquake on the basis of the seismic waveforms recorded at the stations. However, the lead-times can vary depending on the performance of the EEW algorithms adopted. In this study, the regional VS(SC3) system (Behr et al. 2016) was tested by making offline playbacks of the synthetic waveforms. The damage expected at the sites was estimated using a ground motion prediction equation chosen by comparison with the synthetic waveforms.

6.1 Performance of VS(SC3)

The Virtual Seismologist (VS) is a regional EEW methodology that uses a Bayesian approach to predict the likelihood of a given magnitude and source location using incoming data from an on-going earthquake. Prior information, such as network typology, Gutenberg-Richter relationship and past seismicity are used in the assessment (Cua and Heaton 2007). Recently, the VS algorithm was implemented within the SeisComP3 (SC3) framework, which is a full-feature, automated, real-time earthquake monitoring software and represents a community standard software for earthquake detection and waveform processing for regional and global networks across the world. More details about VS(SC3) may be found in Behr et al. (2013, 2016).

VS(SC3) provides near real-time estimates of earthquake magnitude (MVS) as soon as SeisComP3 origins are available, without using prior information in the actual version of the system. Once a SC3 location estimate is available, the VS magnitude estimates can be found with 3-s of P-wave information at a single station. The VS magnitude estimates are then updated every second for a user-defined number of seconds, using additional picks and waveform parameters as they become available.

VS(SC3) was applied to the ground motion scenarios, with a structural velocity model that was computed as the mean of the velocity models used to produce the synthetic seismograms. In case of Barbados, only the intraplate scenarios were analysed, since the number of seismic stations used for the interface earthquakes (i.e. those located within 250 km from the epicentre) was lower than the minimum number required for the estimation of MVS (i.e. six). An example of VS(SC3) performance is given in Fig. 5. The figure illustrates the time trend of the difference between the estimated and real magnitude and hypocentral location, showing that the estimates take a long time to stabilize. This time is larger for the MCEs and for the magnitude estimates and it strongly depends on the network geometry and density of the seismic stations.

Table 6 lists the final difference in magnitude and hypocentre, averaged over the estimates obtained from the 10 source realizations. In general, MVS underestimates the real magnitude, with an average offset of 0.28. The final hypocentral estimate, however, is close to the real one. The worst cases are represented by the MCEs defined for Trinidad, for which an average epicentral difference of about 9–10 km was found, and the intraplate MCE modelled for Antigua, where the depth was estimated with a mean difference of −9.2 km.

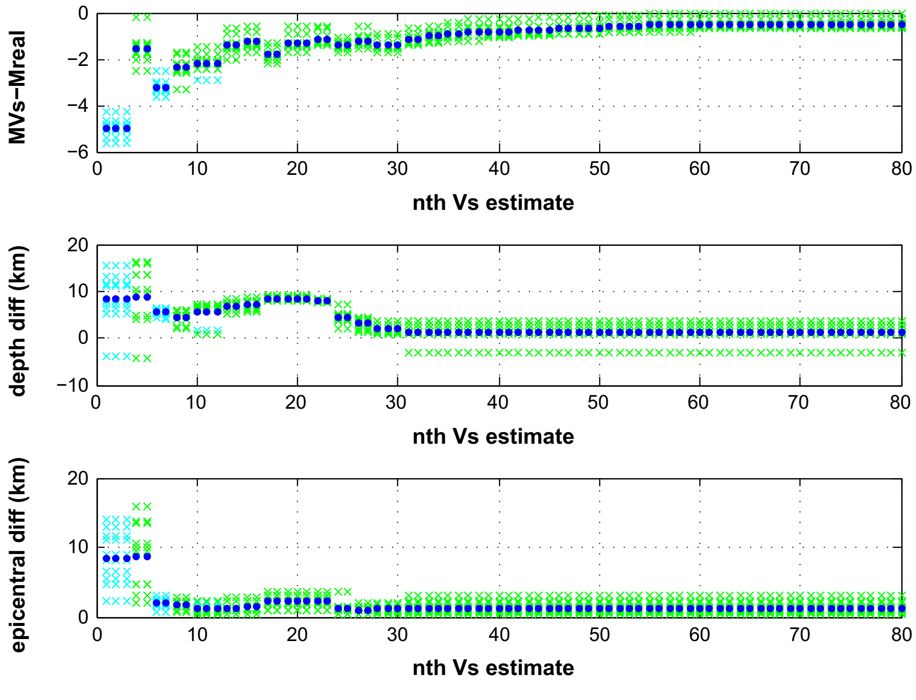

Fig. 5 VS(SC3) performance for the ground motion scenarios associated with the 10 source realizations for Antigua, related to the interface MCE: (*top*) difference between MVS and real magnitude, (*middle*) difference between estimated and real depth and (*bottom*) epicentral difference, updated every second (*green crosses*). The cyan crosses indicate that the VS(SC3) estimate is considered unreliable. The *blue dots* represent the average values

Table 6 VS(SC3) performance: average final difference in magnitude and hypocenter; the standard deviation is given in parenthesis (*F* interface, *P* intraplate, *C* crustal)

Island	Earthquake scenario	MVS-Mreal	Depth diff (km)	Epicentral diff (km)
Antigua	475 years (F)	−0.08 (0.13)	−1.63 (3.41)	2.50 (0.88)
	475 years (P)	−0.47 (0.11)	−1.14 (1.08)	3.77 (0.49)
	MCE (F)	−0.50 (0.22)	1.45 (1.88)	1.33 (0.86)
	MCE (P)	−0.55 (0.10)	−9.20 (1.83)	2.82 (0.91)
Barbados	475 years (P)	−0.40 (0.12)	0.76 (0.60)	2.81 (0.53)
	MCE (P)	−0.25 (0.14)	−0.88 (0.51)	3.44 (0.77)
Trinidad	475 years (C)	0.12 (0.09)	−2.88 (0.08)	0.78 (0.0)
	475 years (P)	−0.37 (0.09)	−0.80 (2.02)	4.27 (0.22)
	MCE (C)	−0.20 (0.13)	−2.97 (2.55)	10.28 (1.67)
	MCE (P)	−0.08 (0.12)	−0.36 (1.28)	9.20 (0.50)

6.2 Selection of GMPEs

The peak ground values determined for the 12 earthquake scenarios modelled using the broadband method by Crempien and Archuleta (2015), were compared with the two GMPEs of Zhao et al. (2006) and Kanno et al. (2006), which were found to provide predictions of ground motions and their variability comparable with those observed in the Lesser Antilles (Douglas and Mohais 2009; Bozzoni et al. 2011). A comparison example is shown in Fig. 6. The maximum horizontal component was used in order to be consistent with the ground motion component adopted for the definition of the damage thresholds. The site class considered is hard rock, which corresponds to a NEHRP (BSSC 2003) site class A. Except for the interface MCE modelled for Antigua, which focus is located near the boundary depth of 30 km used to distinguish between shallow and deep events, the GMPE by Kanno et al. (2006) generally provides a better fit. The GMPE by Kanno et al. (2006) also has the advantage, with respect to Zhao et al. (2006), of being defined in terms of Peak Ground Velocity (PGV), which is the alert response parameter adopted for the National Gas Company of Trinidad and Tobago Ltd pipelines. The comparison in terms of PGV was investigated for Trinidad and it was found to be satisfactory. Therefore, the GMPE by Kanno et al. (2006) was used in conjunction with the results obtained from the application of VS(SC3) algorithm to find the expected damage associated with an on-going earthquake.

6.3 Lead-time and damage associated with VS(SC3) estimates

The lead-time and damage associated with the estimates provided by VS(SC3) were found using the procedure described below. Only the six earthquake scenarios, for which the preliminary analysis (see section Expected damage and theoretical lead-times) supported the installation of an EEW system and the application of VS(SC3) is possible, were taken into account. They are:

- intraplate 475-year return period earthquake, interface and intraplate MCEs for Antigua;
- intraplate 475-year return period earthquake and intraplate MCE for Barbados;
- intraplate MCE for Trinidad.

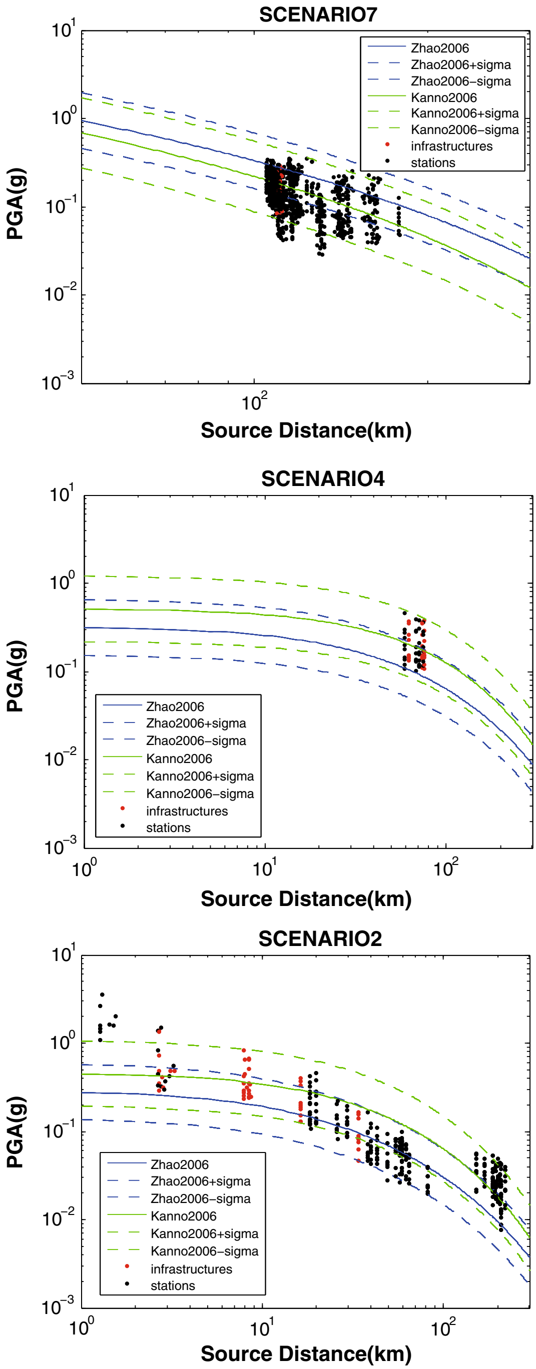

Fig. 6 Comparison of the computed PGAs (*dots*, maximum horizontal) and the GMPEs by Kanno et al. (2006) (*green lines*) and Zhao et al. (2006) (*blue lines*) for: (*top*) the intraplate MCE defined for Antigua, (*middle*) the interface MCE defined for Barbados and (*bottom*) the crustal MCE defined for Trinidad. The *black dots* correspond to the PGAs at the seismic stations, while the *red dots* indicate the PGAs at the sensitive infrastructures. The *solid lines* represent the mean values predicted by the GMPEs, while the *dashed lines* represent the mean values ± one standard deviation. The distance is the minimum distance from the rupture area

For each VS update, the PGA (or PGV for the National Gas Company of Trinidad and Tobago Ltd) expected at the facilities selected was calculated using the GMPE of Kanno et al. (2006), the SC3 location and the VS magnitude (MVS). In order to mitigate the effects due to (a) the long time necessary to stabilize the magnitude estimate and (b) the general underestimation of the final magnitude, the following measures were taken: the mean values predicted by Kanno et al. (2006) increased by one standard deviation were used and MVS was increased by the corresponding offset (0.28). Unreliable VS magnitude estimates (i.e. likelihood <0.99) were excluded.

Besides the magnitude, another parameter with a strong influence on the estimated ground motion is the distance metric adopted. The hypocentral distance can be used only when the earthquakes are regarded as point source, but it is inappropriate for large earthquakes associated with fault ruptures of tens or hundreds of kilometres in length (Bommer et al. 2010; Cauzzi et al. 2014), as applies for the modelled earthquakes. Therefore, an inaccurate estimate of the distance can lead to a severe underestimation of the expected ground motion. In this study, the rupture distance was used and it was determined from the conversion relationship between hypocentral distance and rupture distance proposed by Goda et al. (2010), which was developed starting from a synthetic earthquake catalogue for Western Canada, simulating the fault geometry following the Monte Carlo simulation procedure suggested by Scherbaum et al. (2004) and then calculating different distance measures for a site of interest. This conversion relation is suitable to be used in a real-time automatic-mode since it only requires as input parameters the hypocentral distance and the magnitude of the event, without any a priori knowledge of the rupture geometry. To overcome the problem that this conversion relationship can be used only up to magnitude 7.75 while providing conservative estimates, the rupture distance, decreased by one standard deviation, was used in the GMPE. At the same time, a value of 7.75 was adopted for larger magnitudes. The comparison between the rupture distance computed using the Goda et al. (2010) approach and the real rupture distance is shown in Fig. 7 for some sample facilities.

For each VS update, the estimated peak ground motion value was translated into expected damage by comparison with the damage thresholds for the particular facility (see

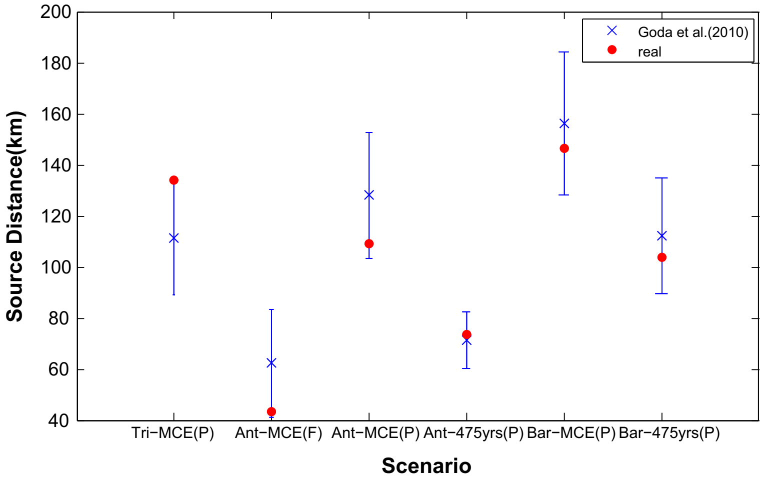

Fig. 7 Comparison between the rupture distance computed with Goda et al. (2010) (average—*blue crosses*, average ± one standard deviation—*blue error bars*) and the real rupture distance (*red circles*) for one sample critical facility for each of the six earthquake scenarios tested with VS(SC3) (*Tri* Trinidad, *Ant* Antigua, *Bar* Barbados, *F* interface, *P* intraplate, *C* crustal)

Table 4). The highest associated damage class was used and the lead-time was found from the difference between the S-wave arrival time at the facility and the time corresponding to the VS update (which can be considered as the time of a virtual alert). Two additional seconds were subtracted in order to take into account the virtual transmission to the processing centre and the virtual transmission of the warning message (Allen 2007). No additional transmission delay, which would be observed if the earthquakes were detected in real-time, was considered.

The procedure was not stopped after an alarm was issued, but was allowed to continue until the VS update coinciding with the S-wave arrival time at the facility. Thus, it was allowed to update the expected damage or terminate the alarm (for example in case of a false alarm determined from the earliest VS estimates).

The results strongly reflect the fact that the initial magnitude estimates are much lower than the final magnitude. In fact, the early predicted ground motion values are generally lower than the threshold associated with the slight damage limit state and this causes the lead-time to be smaller than those in Table 5. For example, for the intraplate 475-year return period earthquake defined for Antigua no lead-time is possible for any source realization, while for the intraplate MCE defined for Trinidad the lead-times vary between 1 and 6.5 s (against the theoretical 10–16 s). For other scenarios, the results vary with the source realization. For example, for the intraplate MCE defined for Antigua, the lead-time for APUA associated with two particular source realizations is almost 13 s, while for other source realizations and facilities, it is only 6 s (the theoretical lead-time is about 15 s). For the intraplate MCE defined for Barbados, the lead-time for the Light & Power Plant associated with some source realizations is 24 s, close to the theoretical lead-time of 25.7 s. However, due to the fact that the magnitudes estimated by VS do not converge monotonically to the correct value (especially the earliest VS updates), the degree of expected damage does not necessarily increase with decreasing lead-time and this may also terminate the alarm, if the expected damage drops below the threshold of the slight damage limit state. As a consequence, the 24 s-alerts associated with the intraplate MCE defined for Barbados last only 3 s and subsequent alerts are generated with a lead-time of 12 s. A similar trend can also be observed in Fig. 8 for the interface MCE defined for Antigua. In this case, the first S-waves reach the sensitive facilities after about 24–25 s from the

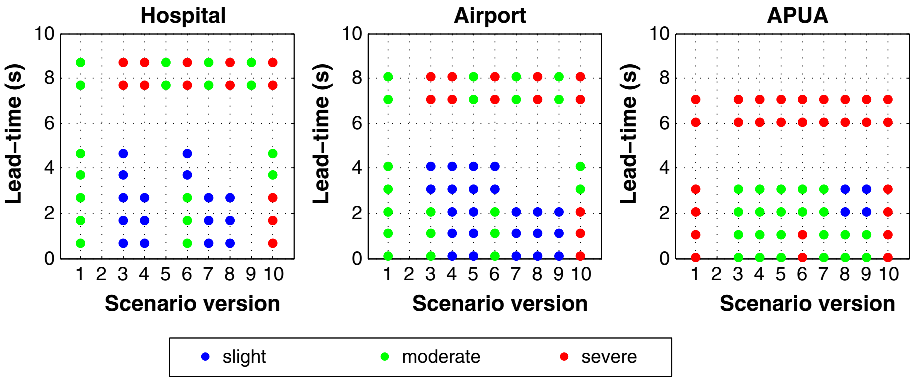

Fig. 8 Lead-time and damage expected from VS(SC3) along with the GMPE by Kanno et al. (2006) for the interface MCE defined for Antigua. The lead-time is given on the y-axis, while the damage is represented by the color. *Each column* correspond to a particular source realization, while *each box* refers to a critical facility

beginning of the rupture. The first magnitude estimates are available 12 s after the beginning of the rupture. Therefore, considering 2 s of technical times, the expected lead-time would be around 10–11 s, consistent with the lead-time given in Table 5. However, from Fig. 5 it is evident that the three first magnitude estimates are considered unreliable. Therefore, the first reliable MVS is available 15 s after the beginning of the rupture, producing an alarm with a lead-time of 7.0–8.7 s, depending on the considered facility, for almost all source realizations. The associated expected damage is severe for APUA and either moderate or severe for the other two facilities, depending on the computed MVS. Only in one case out of 10 (scenario #2) no alarm is issued due to the low MVS estimate (MVS = 6.3). However, the duration of the alarm for the remaining 9 scenarios is of just 2 s due to a decrease of magnitude associated with later estimates. Moreover, MVS estimates are considered unreliable for the next 2 s, therefore producing no lead-time. Afterwards, MVS estimate begins to increase and when the expected PGA exceeds a damage limit state threshold a new alarm is issued with a lead-time of 2–4 s and a degree of expected damage which depends on magnitude and increase with decreasing lead-time (as the magnitude estimate converges to the correct value).

7 Conclusions

This paper presents the results of a feasibility study of an EEW system, which investigated whether such a system could be successfully applied to selected sensitive facilities in the Eastern Caribbean.

In this study, eleven EEW target sites were identified in Trinidad, Barbados and Antigua. The earthquake scenarios for the three islands selected were defined after a thorough analysis of the seismotectonic setting of the Eastern Caribbean region. Two sets of earthquake scenarios were tested for each island: the Maximum Credible Earthquakes (MCEs) and the earthquakes associated with a 475-year return period. Broadband synthetic seismograms (0.1–25 Hz) were produced from the identified earthquake scenarios, both at the sensitive facilities and at the seismic stations in the Eastern Caribbean region. Damage scenarios and shaking alert levels were chosen based on state-of-the-art fragility functions for the selected sensitive facilities. Such seismic fragilities functions were considered both for the response of the single components and for the systemic approach. The curves refer to different limit states and are formulated for various structural systems and building contents. Three-level fragilities were considered to quantify the occurrence of low, moderate and significant damage.

The feasibility study was performed through a two-step analysis.

In the first step, the expected damage was defined from the PGAs (or PGVs for the gas pipelines of the National Gas Company of Trinidad and Tobago Ltd) retrieved from the synthetic seismograms and compared with the theoretical lead-times that could be issued to the selected critical facilities. The theoretical lead-times were estimated for the selected critical facilities simulating both a regional and an on-site EEW configuration. Travel times of P- and S-waves were estimated for the seismic stations and at the critical facilities based on theoretical travel-times. For Antigua and Barbados, results suggest that focus should be placed on an on-site algorithm combined with a regional algorithm. In Trinidad, the simulations performed recommend the installation of a regional EEW system for the strong intraplate seismicity associated with the Paria cluster and suggest further investigations in order to assess the utility of a 2-station trigger regional EEW system to protect facilities from earthquakes generated from the shallow active faults in Trinidad.

In the second step, offline playbacks of VS(SC3) on the synthetic datasets were made in order to evaluate the lead-time and damage associated to this regional EEW algorithm in combination with the GMPE by Kanno et al. (2006), which agrees satisfactorily with the synthetic data. Results showed that the magnitudes and hypocentres estimated by VS(SC3) take a long time to stabilize and the initial magnitude estimates of VS(SC3) are much lower than the final magnitude of the earthquake, which anyway underestimates the real magnitude with an average offset of 0.28. This can be due to the fact that VS(SC3)'s magnitude estimation is based on a likelihood function that was derived empirically for mostly shallow crustal seismicity in California with magnitude $\leq$7.3 (Cua 2005; Cua and Heaton 2007). VS(SC3)'s magnitude estimation relationships assume a depth of 3 km and therefore it is expected that MVS underestimate magnitudes for deep earthquakes. Moreover, a point source approximation is used, which is inappropriate for long ruptures where near-source ground motions are expected even at large distance from the epicenter (Cua and Heaton 2007). As a consequence, the ground motion values initially predicted are generally lower than the thresholds associated with the slight damage limit state and this causes the lead-times to be smaller than those theoretically computed. Moreover, since the magnitudes estimated by VS do not converge monotonically to the correct value (especially the earliest VS updates), the degree of expected damage does not necessarily increase with decreasing lead-time and may also terminate the alarm. Therefore the EEW algorithm tested is unable to provide any stable alert for the modelled earthquake scenarios. To perform better, the Virtual Seismologist likelihood function may need to be re-calibrated for subduction type earthquakes and complemented by an algorithm capable of estimating the finite rupture extent for large earthquakes.

It should be emphasized that the results obtained in this study strongly depend on the network geometry and density of the seismic stations which, in the examined cases, is not optimal due to the peculiarities of the region's geography. Indeed, the Eastern Caribbean is a region largely composed by several small Countries located in the Atlantic Ocean. With the exception of Trinidad, the biggest island, where several active faults were identified on land (although the distances to the strategic sites are too short to allow large operational lead-times), seismicity is dominated by off-shore earthquakes. Thus, independently from the financial resources, the density of the seismic networks could not be significantly improved due to the impracticality of installing off-shore seismic stations. Accordingly, the resources for setting up an efficient EEW system in the Eastern Caribbean should be focused to develop an on-site EEW system combined with a regional EEW that exploit the capabilities of the existing seismic networks.

Acknowledgments The work presented in this paper was supported by the financial contribution of the European Commission within the framework of the FP7 REAKT ("Strategies and tools for Real Time Earthquake RisK ReducTion") Project (grant agreement no. 282862), Working Package 7, Task 7.10 ("Feasibility study of a regional EEW system for the Eastern Caribbean Islands"). The authors would like to acknowledge Mr. Andrea Francia (andreafrancia.it) for the installation and configuration of the Broadband Platform and SeisComP3 (SC3) software packages. They are also grateful to Dr. Jorge Crempien as well as to the guest editor Dr. Carlo Cauzzi and Dr. Yannik Behr for their support in using the Broadband Platform and Virtual Seismologist (SC3) software package, respectively. Finally, a thank is due to the reviewers Dr. Yannik Behr and Dr. Adrien Oth, who contribute to improve the quality of the paper.

References

Allen RM (2007) The ElarmS earthquake early warning methodology and its application across California. In: Manfredi G, Zschau J, Gasparini P (eds) Earthquake early warning systems. Springer, Berlin, pp 21–44

Behr Y, Clinton J, Heimers S, Becker J, Cua G, Cauzzi C, Kaestli P (2013) The virtual seismologist in SeisComp3: system architecture and performance. In: Proceedings of the IAHS-IAPSO-IASPEI joint meeting 2013, Gothenburg, Sweden

Behr Y, Clinton J, Kästli P, Cauzzi C, Racine R, Meier M (2015) Anatomy of an earthquake early warning (EEW) alert: predicting time delays for an end-to-end EEW system. Seismol Res Lett 86:830–840. doi:10.1785/0220140179

Behr Y, Clinton J, Cauzzi C, Hauksson E, Jónsdóttir K, Marius C, Pinar A, Salichon J, Sokos E (2016) The virtual seismologist in SeisComP3: a new implementation strategy for Earthquake Early Warning algorithms. Seismol Res Lett, in press

Bengoubou-Valerius M, Bazin S, Bertil D, Beauducel F, Bosson A (2008) CDSA: a new seismological data center for the French Lesser Antilles. Seismol Res Lett 79(1):90–102

Blaser L, Krüger F, Ohrnberger M, Scherbaum F (2010) Scaling relations of earthquake source parameters estimates with special focus on subduction environment. Bull Seismol Soc Am 100(6):2914–2926

Bommer JJ, Douglas J, Scherbaum F, Cotton F, Bungum H, Faeh D (2010) On the selection of ground-motion prediction equations for seismic hazard analysis. Seismol Res Lett 81(5):783–793

Böse M, Wenzel F, Erdik M (2008) PreSEIS: a neural network-based approach to earthquake early warning for finite faults. Bull Seismol Soc Am 98(1):366–382

Bozzoni F, Corigliano M, Lai CG, Salazar W, Scandella L, Zuccolo E, Latchman J, Lynch L, Robertson R (2011) Probabilistic seismic hazard assessment at the eastern caribbean Islands. Bull Seismol Soc Am 101(5):2499–2521

BSSC—Building Seismic Safety Council (2003) NEHRP recommended provisions for seismic regulations for new buildings and other structures (FEMA 450), Washington, USA

Cauzzi C, Faccioli E, Vanini M, Bianchini A (2014) Updated predictive equations for broadband (0.01–10 s) horizontal response spectra and peak ground motions, based on a global dataset of digital acceleration records. Bull Earthq Eng 13:1587–1612. doi:10.1007/s10518-014-9685-y

Chaudhuri S, Hutchinson T (2006) Fragility of bench-mounted equipment considering uncertain parameters. J Struct Eng, ASCE 132(6):884–898

Chong WH, Soong TT (2000) Sliding fragility of unrestrained equipment in critical facilities. Multidisciplinary Center for Earthquake Engineering Research (MCEER) Technical Report, Buffalo, USA

Crempien JGF, Archuleta RJ (2015) UCSB method for broadband ground motion from kinematic simulations of earthquakes. Seismol Res Lett 86(1):61–67

Crosby CJ, Prentice CS, Weber JC, Ragona D (2009) Logs of paleoseismic excavations across the Central Range fault, Trinidad, US Geological Survey Open-File Report 2009–1228, Plates 1 and 2

Cua G (2005) Creating the virtual seismologist: developments in ground motion characterization and seismic early warning. Ph.D. thesis, California Institute of Technology

Cua G, Heaton T (2007) The virtual seismologist (VS) method: a Bayesian approach to earthquake early warning. In: Gasparini P, Manfredi G, Zschau J (eds) Seismic early warning. Springer, Heidelberg, pp 85–132

Douglas J, Mohais R (2009) Comparing predicted and observed ground motions from subduction earthquakes in the Lesser Antilles. J Seismol 13(4):577–587

Feuillard M (1985) Macrosismicité de la Guadeloupe et de la Martinique. Ph.D. Thesis, Institut de Physique du Globe de Paris, Paris

Feuillet N, Beauducel F, Tapponnier P (2011) Tectonic context of moderate to large historical earthquakes in the Lesser Antilles and mechanical coupling with volcanoes. J Geophys Res 116:B10308

Goda K, Hong HP, Atkinson GM (2010) Impact of using updated seismic information on seismic hazard in western Canada. Can J Civ Eng 37(4):562–575

González OF, Alvarez JL, Moreno B, Panza GF (2012) S-wave velocities of the lithosphere–asthenosphere system in the caribbean region. Pure appl Geophys 169(1):101–122

Goodwin E, Maragakis E, Itani A (2004) Seismic evaluation of hospital piping systems. In: Proceedings of the 13th world conference on earthquake engineering, Vancouver, BC, Canada, Paper no 1081

Grases J (1990) Terremotos destructores del Caribe 1502–1990. Una contribución al Decenio Internacional para la Reducción de los Dessastres Naturales. Caracas: UNESCO—RELACIS

Gutscher M, Westbrook GK (2009) Great earthquakes in slow-subduction, low-taper margins. In: Lallemand and Funiciello (eds) Subduction zone geodynamics (frontiers in earth sciences), pp 119–133

Herrmann RB (2003) Computer programs in seismology, open files. http://www.eas.slu.edu/People/RBHerrmann/CPS330.html. Accessed Dec 2012

Kanamori H (2005) Real-time seismology and earthquake damage mitigation. Ann Rev Earth Planet Sci 33(1):195–214

Kanno T, Narita A, Morikawa N, Fujiwara H, Fukushima Y (2006) A new attenuation relation for strong motion in Japan based on recorded data. Bull Seismol Soc Am 96(3):879–897

Kennett BLN, Engdahl ER, Buland R (1995) Constraints on seismic velocities in the Earth from travel times. Geophys J Int 122(1):108–124
Köhler N, Cua G, Wenzel F, Böse M (2009) Rapid source parameter estimations of southern california earthquakes using PreSEIS. Seismol Res Lett 80(5):748–754
Konstantinidis D, Makris N (2009) Experimental and analytical studies on the response of freestanding laboratory equipment to earthquake shaking. Earth Eng Struct Dyn 38(6):827–848
Lanzano G, Salzano E, Santucci de Magistris F, Fabbrocino G (2013) Seismic vulnerability of natural gas pipelines. Reliab Eng Syst Saf 117:73–80
Ludwig WJ, Nafe JE, Drake CL (1970) Seismic refraction. In: Maxwell AE (ed) The sea, vol 4. Wiley, New York, pp 53–84
Meier MA, Heaton T, Clinton J (2015) The gutenberg algorithm: evolutionary Bayesian magnitude estimates for earthquake early warning with a filter bank. Bull Seismol Soc Am 105(5):27742786
O'Rourke M, Deyoe E (2004) Seismic damage to segmented buried pipe. Earthq Spectra 20(4):1167–1183
O'Rourke M, Liu X (1999) Response of buried pipelines subjected to earthquake effects. MCEER Monograph No. 3, University of New York Buffalo
Olsen KB, Mayhew JE (2010) Goodness-of-fit criteria for broadband synthetic seismograms, with application to the 2008 Mw5.4 Chino Hills, CA, Earthquake. Seismol Res Lett 81(5):715–723
Olsen KB, Day SM, Bradley CR (2003) Estimation of Q for long-period (2 sec) waves in the Los Angeles Basin. Bull Seismol Soc Am 93(2):627–638
Pindell JL, Kennan L (2009) Tectonic evolution of the Gulf of Mexico, Caribbean and northern South America in the mantle reference frame: an update. Geol Soc London Spec Publ 328:1–55
Pindell J, Kennan L, Maresch WV, Stanek K, Draper G, Higgs R (2005) Plate-kinematics and crustal dynamics of circum-Caribbean arc-continent interactions: tectonic controls on basin development in proto-Caribbean margins. Spec Pap Geol Soc Am 394:7–52
Pitilakis K, Crowley H, Kanya A (2014) SYNER-G: typology definition and fragility functions for physical elements at seismic risk geotechnical. Geol Earthq Eng 27
Porter KA, Kiremidjian AS (2001) Assembly-based vulnerability of buildings and its uses in seismic performance evaluation and risk-management decision making. Report no. 139, John A Blume Earthquake Engineering Research Center, Stanford, CA
Prentice CS, Weber JC, Crosby CJ, Ragona D (2010) Prehistoric earthquake on the Caribbean-South American plate boundary, Central Range fault, Trinidad. Geology 38(8):675–678
Retamales R, Mosqueda G, Filiatrault A, Reinhorn AM (2008) Experimental study on the seismic behaviour of non-structural components subjected to full-scale floor motions. In: Proceedings of the 8th US national conference on earthquake engineering, USA
Russo RM, Speed RC, Okal EA, Shepherd JB, Rowley KC (1993) Seismicity and tectonics of the Southeastern Caribbean. J Geophys Res 98(B8):14299–14319
Salazar W (2012) Strong motion database—Eastern Caribbean Islands. REAKT Project. The University of the West Indies, St. Augustine
Salazar W, Brown L, Mannette G (2013) Probabilistic seismic hazard assessment for Bridgetown–Barbados, employing subduction interface characteristic earthquakes. J Civil Eng Arch 7(11):1405–1422
Satriano C, Lomax A, Zollo A (2008) Real-time evolutionary earthquake location for seismic early warning. Bull Seismol Soc Am 98(3):1482–1494
Scherbaum F, Schmedes J, Cotton F (2004) On the conversion of source-to-site distance measures for extended earthquake source models. Bull Seismol Soc Am 94(3):1053–1069
Schmedes J, Archuleta RJ, Lavallée D (2013) A kinematic rupture model generator incorporating spatial interdependency of earthquake source parameters. Geophys J Int 192(3):1116–1131
Shepherd JB (1992) Comment on "Subduction and seismic hazard in the Lesser Antilles" by Pascal Bernard and Jerome Lambert. Bull Seismol Soc Am 82(3):1534–1543
Soto MD, Mann P, Escalona A, Wood LJ (2007) Late Holocene strike-slip offset of a subsurface channel interpreted from three-dimensional seismic data, eastern offshore Trinidad. Geology 35(9):859–862
Strasser FO, Arango MC, Bommer JJ (2010) Scaling of the source dimensions of interface and intraslab subduction-zone earthquakes with Moment Magnitude. Seismol Res Lett 81(6):941–950
Tromans I (2004) Behavior of buried water supply pipelines in earthquake zones. Ph.D. Thesis, Imperial College of Science, Technology and Medicine, University of London
Weber JC (2009) Neotectonics in the Trinidad and Tobago, West Indies segment of the Caribbean-South American plate boundary. Occasional Papers of the Geological Institute of Hungary, volume 204
Weber J, Dixon TH, DeMets C, Ambeh WB, Jansma P, Mattioli G, Saleh J, Sella G, Bilham R, Perez O (2001) GPS estimate of the relative motion between the Caribbean and South American plates, and geologic implications for Trinidad and Venezuela. Geology 29(1):75–78

Wells DL, Coppersmith KJ (1994) New empirical relationships among magnitude, rupture length, rupture width, rupture area and surface displacement. Bull Seismol Soc Am 84(4):974–1002

Wu Y-M, Kanamori H (2005) Experiment on an onsite early warning method for the taiwan early warning system. Bull Seismol Soc Am 95(1):347–353

Zhao JX, Zhang J, Asano A, Ohno Y, Oouchi T, Takahashi T, Ogawa H, Irikura K, Thio HK, Somerville PG, Fukushima Y, Fukushima Y (2006) Attenuation relations of strong ground motion in Japan using site classification based on predominant period. Bull Seismol Soc Am 96(3):898–913

Zollo A, Amoroso O, Lancieri M, Wu YM, Kanamori H (2010) A threshold-based earthquake early warning using dense accelerometer networks. Geophys J Int 183(2):963–974